Radar Velocity Analysis in Studying the Barrier Island Sediments of Robert Moses State Park

Taylor Grandfield and Dan Davis
taylor.grandfield@stonybrook.edu
daniel.davis@stonybrook.edu
Department of Geosciences, Stony Brook University

As part of an ongoing project to understand better the evolution of a highly dynamic barrier island system, we have recently carried out a series of Common Midpoint (CMP) Ground Penetrating Radar (GPR) surveys in Robert Moses State Park on Fire Island, NY. This work complements an earlier series of zero/constant-offset imaging GPR studies by constraining radar velocities and, thus, the vertical scale of the GPR imaging we use for studying the island's stratigraphy and rapid evolution.

As described by Komar (1998), barrier islands are elongated, shore-parallel masses of unconsolidated sediment, sand or gravel, extending above the high tide level and separated from the mainland by a lagoon or marsh (Figure 1). GPR can be useful in studying a barrier island because its growth and erosion are recorded in the sedimentary record that is well imaged using GPR.

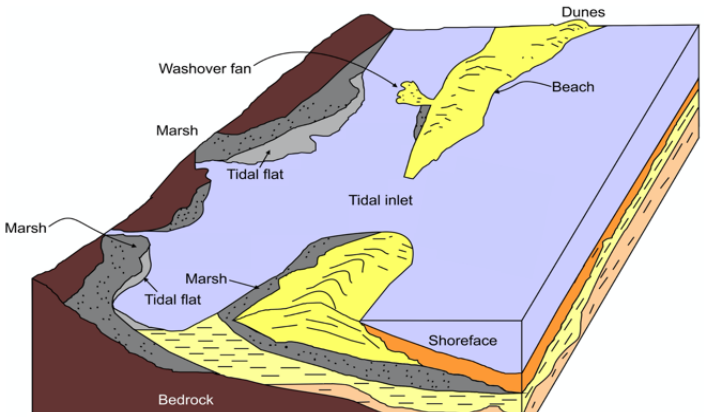

Figure 1. Schematic cross-section of a barrier island. The rock beneath the mainland is depicted in dark brown, although in the case of Long Island true bedrock is far deeper. The gray areas are marshy deposits, which are typically formed in lower energy environments, such as within the Great South Bay. The upper yellow layer in the barrier island consists of dunes and sandy beach sediments facing the ocean. Ongoing storm activity causes features such as tidal inlets and wash-over fans to form. When sea level was lower the entire system would have been centered farther south. As sea level rises the system migrates towards the north. After Cooper et al. (2018).

Fire Island is a barrier island located at an average distance of about 5 km from the southern shore of Long Island. It has a documented history of westward growth, punctuated by storm-related erosional events, as along shore currents transport sediment westward from the bluffs located on the south shore eastern Long Island. Our surveys were carried out near the westernmost tip of Fire Island, in Robert Moses State Park (RMSP).

Shallow geophysical techniques, such as GPR, are used in nonintrusive surveys to analyze the near subsurface. GPR at RMSP allows an analysis of erosional and depositional surfaces that records Fire Island's recent geologic history. At present, we are pairing data from GPR surveys with drilling data and bathymetric maps in order to ground truth our findings. To do this, however, requires knowing the vertical scale in GPR imagery with depth, and that requires good constraints on the velocity of radar propagation. This is why we have undertaken the CMP surveys described here. Our ultimate goal is to understand better the history of the erosional events and rapid deposition within this barrier island system.

This survey focuses on the golf course located at Robert Moses State Park field 2, near the westernmost end of the park. Figure 2A depicts the location of RMSP on Long Island and the rectangular box corresponds to the area depicted in Figures 2B and 2C. In those figures, the RMSP field 2 golf course is outlined by a red rectangle and the location of the Fire Island lighthouse is indicated by a red star. Together, a bathymetric map from 1851 (Figure 2B) and composite of aerial images from 1994 (Figure 2C) record the island's 7 km westward growth and rapid sediment deposition over those 143 years. These events are recorded within the stratigraphic record and, as long as the sediments do not contain salty pore water (the electrical conductivity of which impedes radar signals), they can be imaged through GPR surveys. Our previous GPR surveys at the golf course (Grandfield and Davis, 2020) created a 23x90m grid, with 24 parallel lines of 90m in length. In addition to the main lines, 3 horizontal crosslines were taken perpendicular to the main lines in areas of few surface obstructions.

Ground Penetrating Radar (GPR) is a geophysical technique for imaging the subsurface using a transmitting antenna that emits a radio-frequency signal and a receiving antenna that records the part of the signal that returns to the surface after it has been reflected and scattered off of layers and objects in the subsurface (Neal 1998).

Energy returned from deeper layers and objects are recorded by the receiver at later times than from shallower layers. Although the horizontal axis of a GPR image is horizontal distance (in m) the vertical axis is therefore time in nanoseconds (ns), rather than depth in meters. Sedimentary layers can produce strong GPR reflectors when vertical changes in the packing, water saturation or mineralogy of the sediments, all of which can produce contrasts in radar velocity. This makes GPR a potent tool for studying the stratigraphy of sedimentary systems (e.g., Buynevich et al., 2008). There are two main types of survey techniques: Common Offset (CO) and Common Midpoint (CMP).

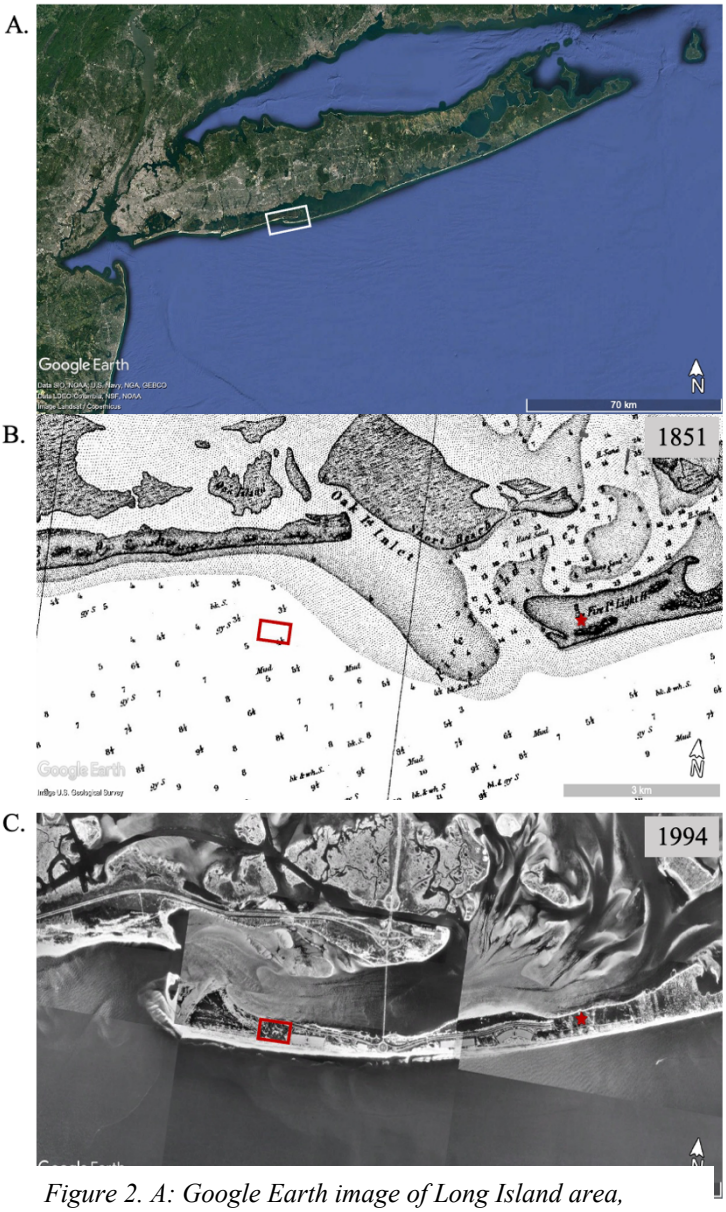

Figure 2. A: Google Earth image of Long Island area, showing area covered by 1851 map and 1994 aerial images (B and C, respectively).

Common Offset GPR surveys are the most common setup used. As depicted in Figure 3, they consist of a transmitter (Tx) and a receiver (Rx) that move across the surface with a constant (and usually quite small) separation from each other. Signal is reflected and scattered off of buried objects and collected by the receiver. It is then processed to remove a variety of undesired data artifacts.

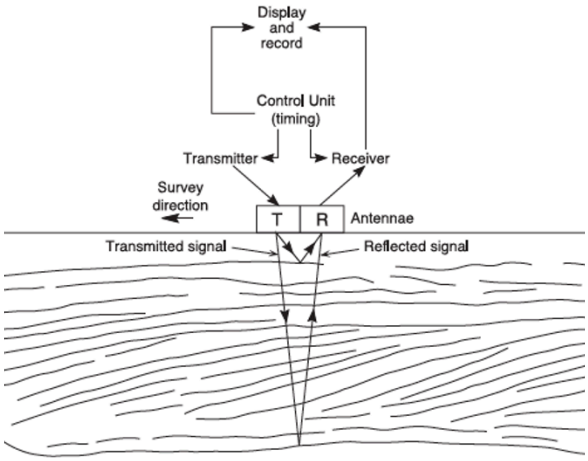

Figure 3. Schematic diagram of the acquisition of a single data trace in a common offset (sometimes called zero-offset) GPR survey. Signals sent by a transmitting antenna are collected by a receiving antenna kept at a small, fixed distance from it. The antenna pair is moved across the surface, and the individual data traces combine to form a radargram (a raw radar image of the subsurface). The operator reviews the raw data on a monitor as it is stored in the control unit for later processing back in the lab (Annan 2003).

The depth to a subsurface layer imaged using GPR is recorded by the receiving antenna in terms of the time it took for the energy to travel from the transmitter to the layer, reflect off of the layer, and travel back to the receiver - this is also known as the two-way travel time. To obtain correct depths of reflectors within the radargram requires the conversion from time to distance, and that requires knowing the radar velocity. When the area has topographic relief, it must also be accounted for if the geometry of radar reflectors are to be imaged properly. The need to do this is another reason why it is necessary to know the radar propagation velocity in the medium being imaged.

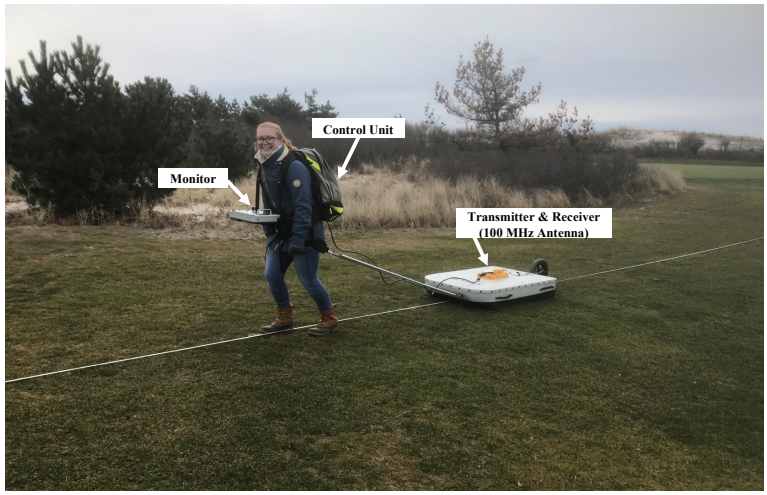

Figure 2. Field example of common offset data acquisition, using a sled setup with a 100MHz antenna on the RMSP Golf Course grid (Grandfield and Davis 2020).

Electromagnetic waves in air travel at essentially the same velocity as in a vacuum ($c \approx 30$ cm/ns). In a material that is non-magnetic and non-conducting, that velocity drops proportionally with the square root of the relative permittivity (dielectric constant). Geologically relevant velocities can range from about 15 cm/ns in dry, porous sand to about 6 cm/ns in clays (Annan, 2003). Generally, on Long Island the subsurface includes glacial till containing large, buried clasts that the radar ray diffracts off of leading to hyperbolas, 'frowns', in the resulting radargram. These diffraction hyperbolas can be analyzed through using GPR processing software, in our case *Reflexw*, to fit the shape of the hyperbolas and thereby determine the radar velocity. In a barrier island setting, however, there are typically no large, deep clasts to produce such diffraction hyperbolas. This requires another method to determine the velocity structure.

Figure 5 displays a 250 MHz radargram, with our geologic interpretations, from the westernmost (X=0) south-north main line in the RMSP Golf Course grid (Grandfield and Davis, 2020). Note that in addition to shallow anthropogenic objects (e.g., pipes), our survey imaged the water table, low angle depositional surfaces, and erosional surfaces that were likely formed as a result of storm erosion during the overall growth of the island.

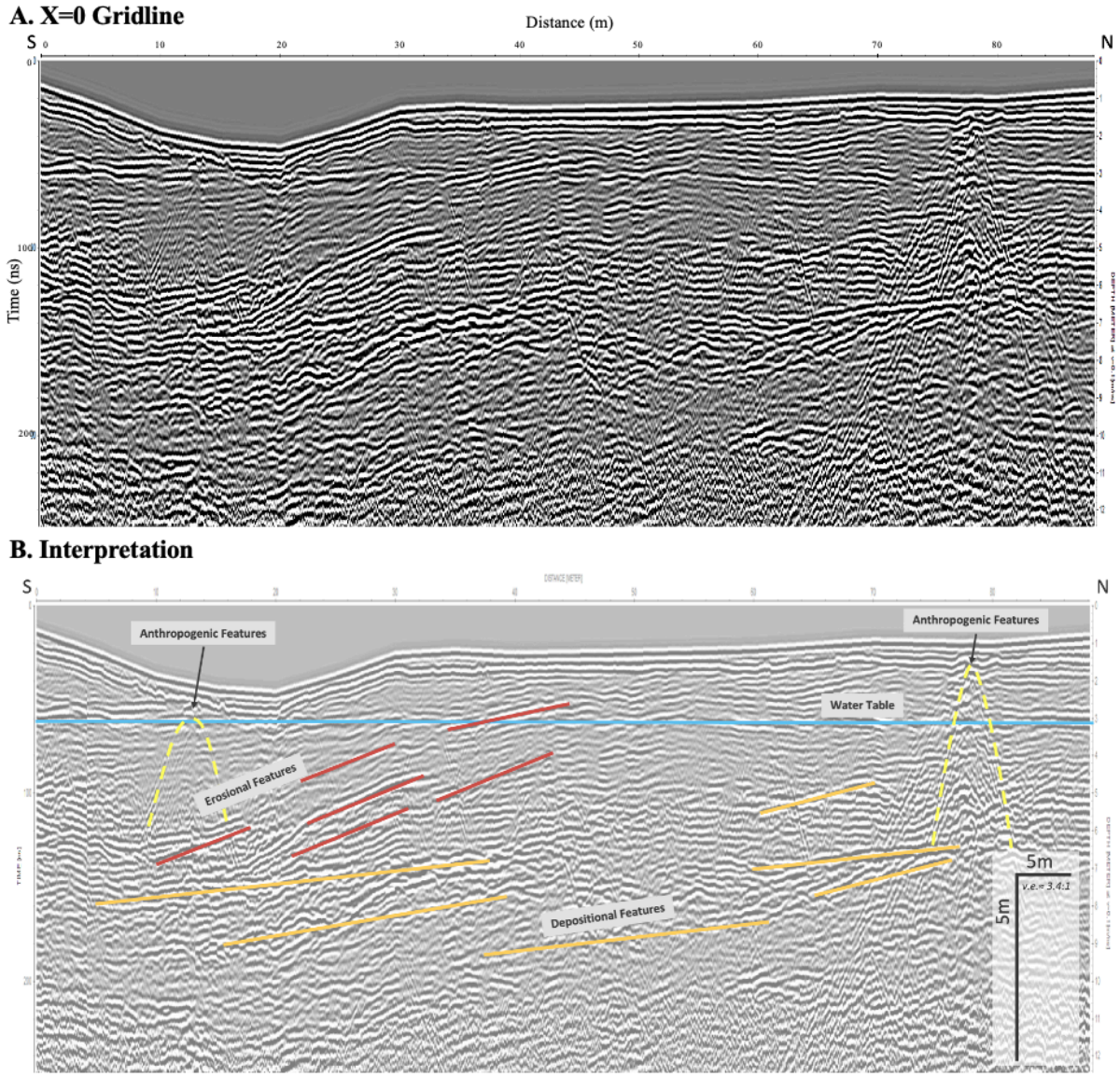

Figure 3. Example of processed data with interpretations taken from a CO GPR survey. A is a processed radargram collected at the RMSP golf course with a 250 MHz antenna. B contains our interpretation of the radargram shown in A. The horizontal reflector, in blue, corresponds to the water table. The reflectors in red are interpreted to be erosional features: their dips average about 7°. The reflectors highlighted in orange, dipping about 2°, are interpreted to be depositional layers. The hyperbolas, in yellow, are diffractions within the shallow surface. These are caused by isolated objects, in this case anthropogenic features related to the sprinkler system and associated pipes within the golf course.

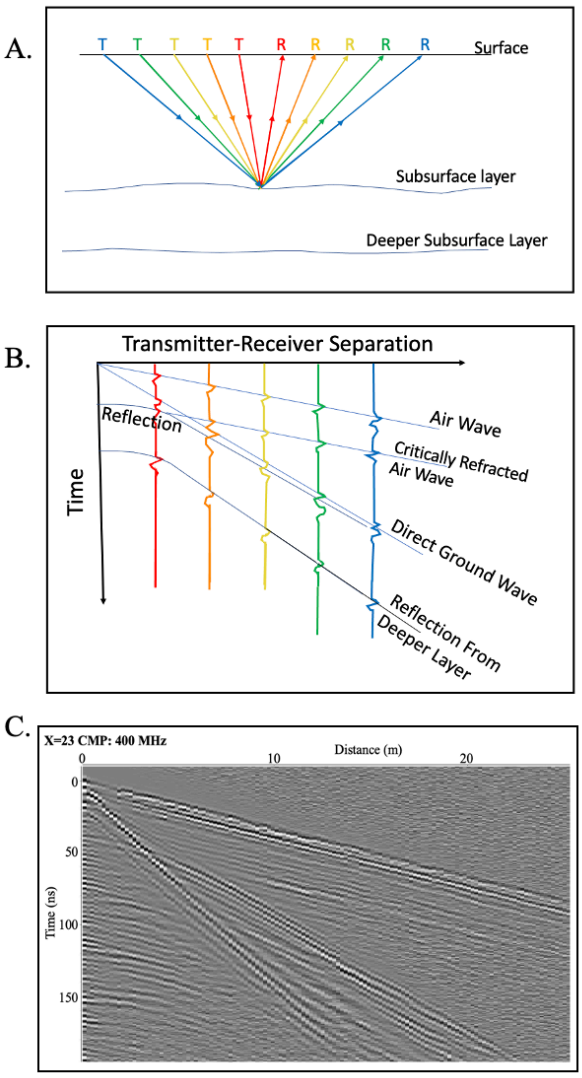

Figure 7 (above). CMP survey geometry and data: A symmetric set of ray paths (A) produce direct and reflected waves (B) that can be used to determine the effective radar velocities and thus the depths to subsurface layers. Example data from the RMSP golf course grid X=23 line are shown in C. A and B are modified after Baker and Jol (2007).

Figure 8 (at right). The CMP data displayed in Figure 7C with hand-picked fits to the hyperbolae, shaded with color to highlight the picked hyperbolas/velocity picks. Note the gradual decrease in the measured velocities for each hyperbola-producing radar-reflective layer.

Figure 4. Data acquisition at X=23 grid line at the RMSP golf course. CMP setup using 400 MHz bistatic unshielded antennas.

We have augmented our common offset data with common-midpoint (CMP) surveys. In a CMP survey the transmitting and receiving antennas are moved symmetrically away from a constant central point, so that regardless of their separation distance the point of signal reflection on any buried layer remains fixed (Figure 7A). The result is a series of air, ground, and reflected waves analogous to those produced in similar seismic surveys, with the important distinction that for GPR, air is the fastest, rather than the slowest, medium (Figure 7B). CMP data from the X=23m line in the golf course grid is shown in Figure 7C.

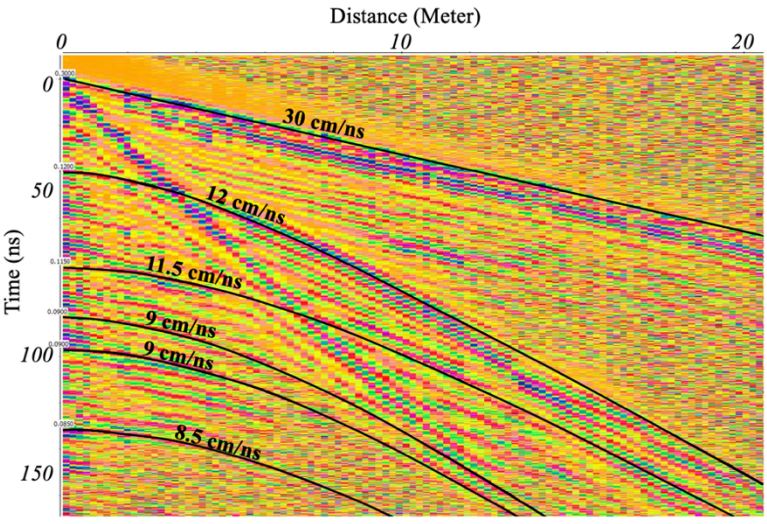

Velocity estimates can be determined from CMP surveys in two ways: manual hyperbola fitting and semblance analysis. Manual fitting allows us to fit hyperbolas by eye with a combination of velocity and time that match the hyperbolic signal within the CMP data, as seen in Figure 8. Semblance is a process that does this quantitatively by determining the degree to which energy from the CMP data is consistent with each possible combination of velocity and time. Pairing these two methods with survey data from different frequencies allows us to create the best estimate of radar velocities for the survey location. Figure 9, below, displays semblance analysis results for 200 MHz and 400 MHz bistatic unshielded antennas in golf course grid line X=23.

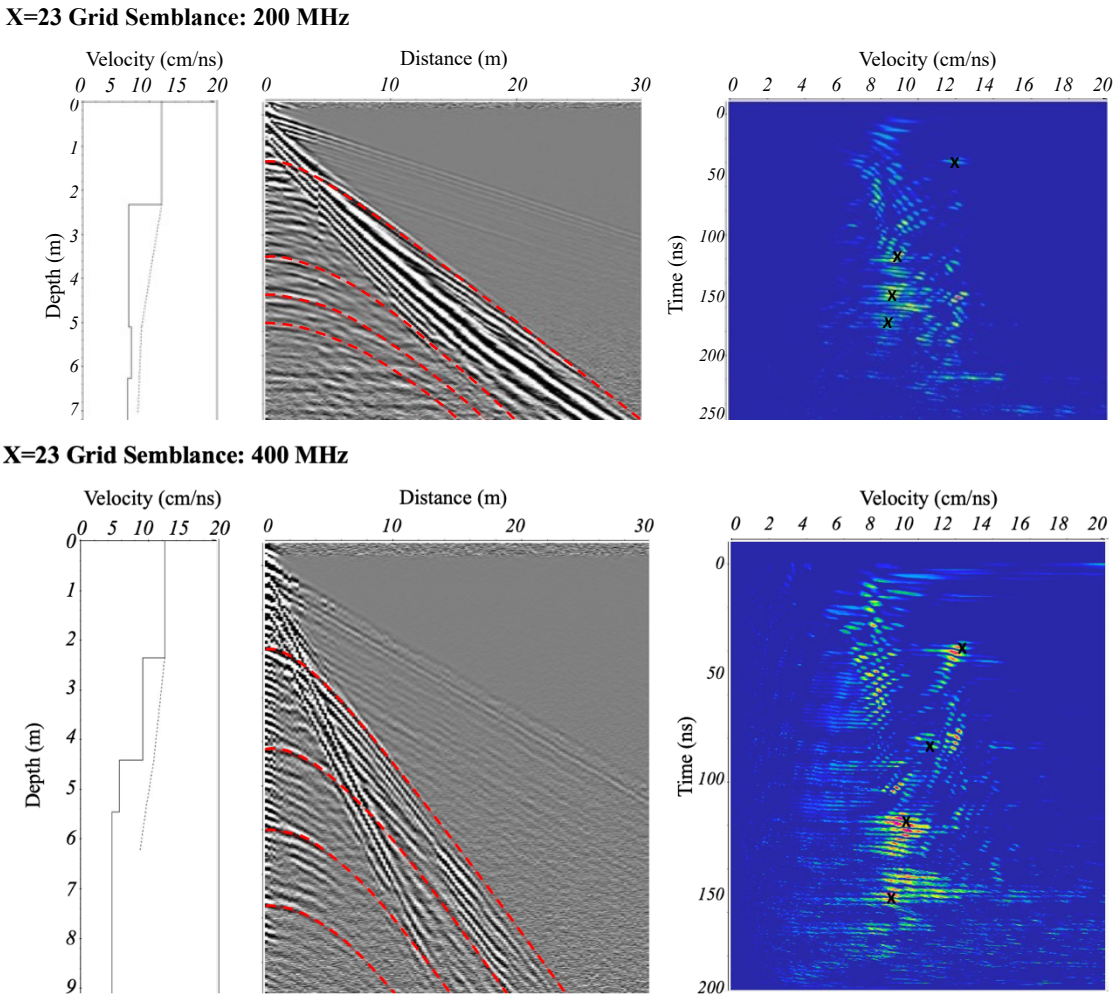

Figure 9. Semblance analysis for X=23 grid line CMP data (200 MHz at top and 400 MHz below that). In each case, the middle image is the CMP data plot with hyperbolas fit (in red) according to the results of the semblance analysis, shown at right. The solid line in the plot at left displays the velocity model. That, in turn, defines the measured effective velocity as a function of depth. This is different than the velocity at that depth: instead, it corresponds to the inverse of the mean slowness (inverse velocity) to that depth. The bright spots in the semblance plot at right correspond to strong indications of the effective velocity for the reflector at that time/depth. The black X marks correspond to areas of bright spots that were used to create the model at left. In this case the semblance analysis for the two frequencies show complementary results with faster velocities, around 12cm/ns, near the surface. This is interpreted to be due to the bulk of those ray path lengths being in unsaturated sediments. As we get into areas where the ray paths spend more time in saturated sediments, we see velocities between 9-10 cm/ns at around 100 ns and an overall trend of decreasing velocities with increasing time/depth.

Once the general velocity structure was determined through analysis of CMP data, we then tested our velocities on the golf course grid lines by applying a migration to the golf course grid CO survey data. Migration redistributes energy within individual traces within the radargram from the region below where the trace was generated to the area that it originated (e.g., Annan, 2003). Migration with incorrect velocity estimates will not collapse energy into a point region but will instead add additional non-physical artifacts. With correct velocity assumptions, however, migration will collapse energy into its points of reflection, in turn increasing resolution and placing features at their correct locations and dip angles. The ultimate goal of migration is to make the radargram look as geologically and structural accurate as possible (Neal, 2004).

Successful migration can serve as a verification of the velocity structure determined from a CMP GPR survey. Migration with correct velocities should collapse hyperbolas and tighten up radar reflectors (e.g., Figure 10C). They should also allow for better depth estimates and dip angles, which in turn gives us a better idea of the local stratigraphy. Errors in migration are easily identifiable and can give additional information about the velocity structure within the radargram. When migration is used with velocities that are too slow the diffraction hyperbolas do not collapse (e.g., Figure 10B), but when the velocity used is too fast the opposite occurs and 'smiles' are added to the radargram (e.g., Figure 10D).

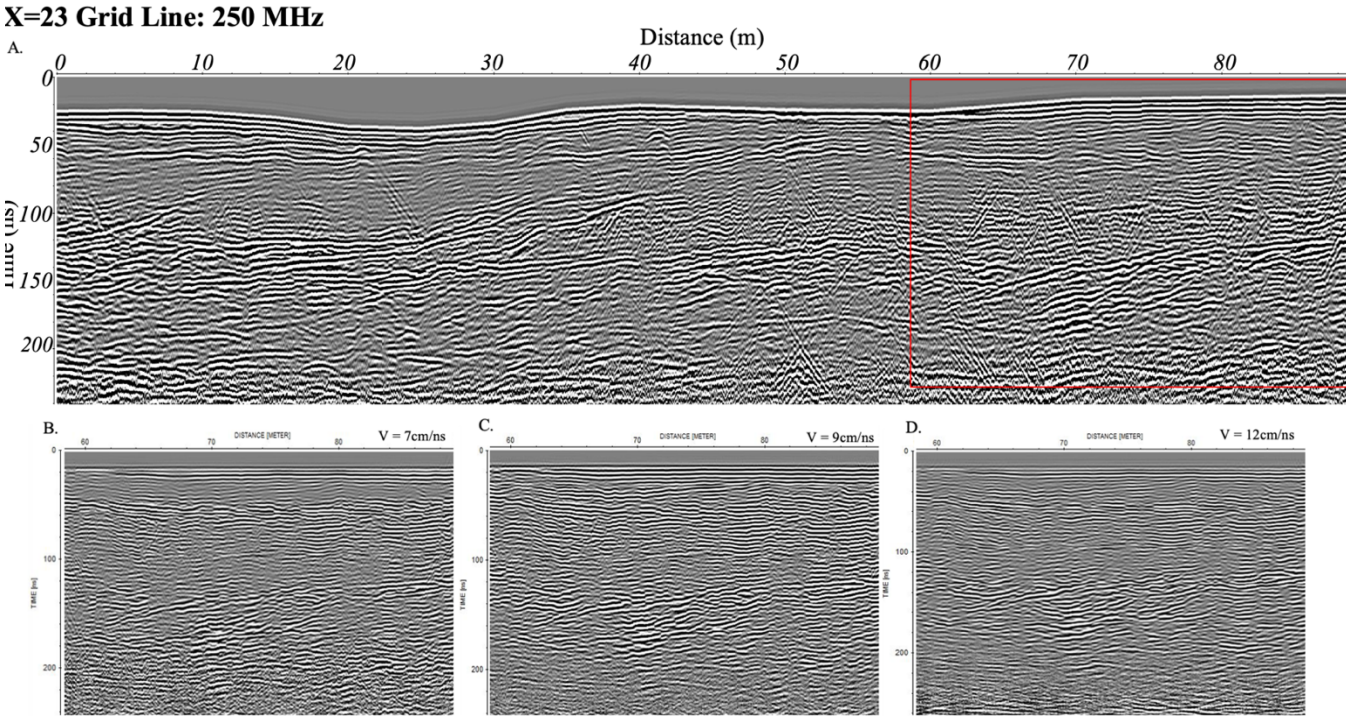

Figure 10. Example use of migration for the golf course grid X=23 line, collected through a CO survey. A is a processed, unmigrated radargram collected with a 250 MHz antenna. The red rectangle outlines the location of the CMP surveys on the X=23 gridline and corresponds to the area focused on in B-D. B is migrated with a velocity of 7cm/ns, too slow for majority of the radargram. The slow chosen velocity does not remove diffraction hyperbolas towards the top of imaging, but towards the bottom it is closer to the correct velocity. C is migrated with a velocity of 9 cm/ns, although it is a bit slow for the very shallow (top 20 ns) of the radargram, this velocity is likely, within 5%, of the best overall velocity for the region. As displayed in C, diffraction hyperbolas have been collapsed and there is a clearer idea of the stratigraphy. D is migrated with a velocity that is too fast, 12cm/ns. This velocity may be appropriate for the very top of the radargram, but is fast for the rest causing the 'smiles' found towards the center of D.

We have obtained drilled samples to a depth of 40' in a picnic area adjacent to the RMSP golf course (Figure 11). Although we had previously run a set of CO GPR surveys there, the radar velocity was not well enough constrained to make it possible to try to correlate core samples with GPR reflectors. Therefore, in January 2021, we collected CMP data over the drill site location using 200 and 400 MHz unshielded bistatic antennas. The 200 MHz antenna provides deeper penetration with moderate resolution, while the 400 MHz antenna provides very good shallow resolution with less penetration depth.

Figure 11. Drilling at the RMSP Field 2 Picnic Area in April 2019. Vesna Kundic and Jeonghyeop (Jey) Kim for scale.

Semblance analysis of the 200 MHz data (Figure 12A) indicates a high velocity (≈12 cm/ns) within much of the top 100 ns, becoming much slower over the second hundred ns. Deeper, the velocity is much lower. The 400 MHz CMP data (Figure 12B) provides higher resolution, indicating velocities as high as 14 cm/ns near the surface and about 12 cm/ns to about 75 ns. That time-velocity combination corresponds to about 4.5 meters (15'). This is consistent with the dry sandy nature of the site (Figure 11). We know from previous surveys (Girardi and Davis, 2010; Itzkin, 2016) that dry sand can be very radar-fast. Both CMP analyses indicate that the velocity is lower at greater depth: 8 cm/ns at 200 ns corresponds to a depth of 8 meters (≈26'), by which depth the drilled samples were much tighter and resistant to drilling (with high drill count). This velocity profile is consistent with saturated sediments below the water table and the clayey sediments found within deeper drill samples.

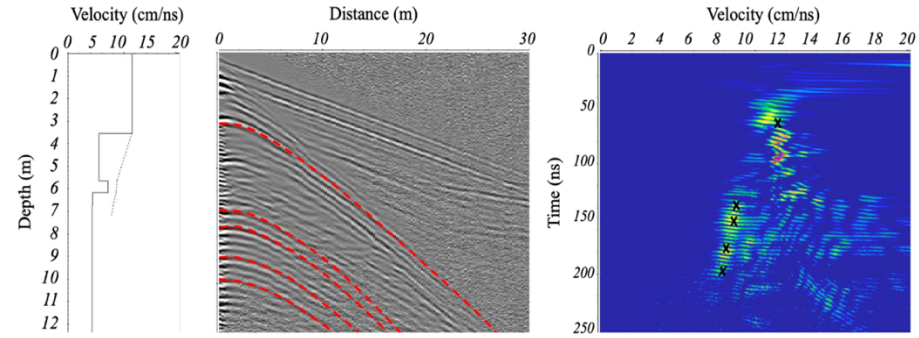

Figure 12A.

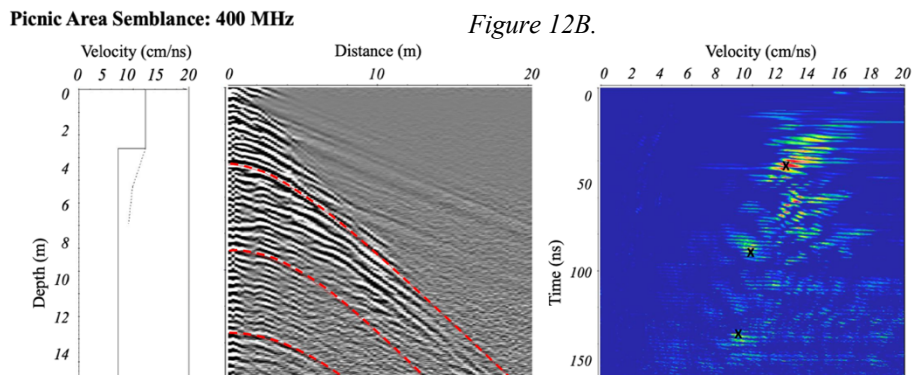

Figure 12B.

Figure 12
A (top): Semblance analysis of 200 MHz CMP survey at RMSP drilling site (Fig. 11).
B (bottom): Similar analysis of 400 MHz CMP survey there.
A very high velocity of ≈14 cm/ns over the top 35 ns or so would be match the observed water table depth of 8' (2.4 m).
A velocity of 8 cm/ns to 200 ns corresponds to a depth of 8 m (≈26'), where drilling shows wet, compacted, and muddier sediment.

Previous studies (e.g., Itzkin, 2016) have demonstrated the potential of using GPR as a tool in understanding the recent geologic history of barrier islands such as Fire Island. Here, we have demonstrated the need to constrain radar velocity in order to scale GPR data properly with depth and correlate GPR imagery with drilling data, as well as the potential of properly migrated GPR lines to aid in stratigraphic analysis. In the near future, we plan to continue the migration of RMSP golf course grid CO GPR data (Grandfield and Davis, 2020), in order to understand better the southward dipping reflectors that record the deposition and erosion of sediment. With new constraints on radar velocity and the true depth to reflectors we will be able to place drilling samples in context, including deeper reflectors that we believe to be marsh sediments predating the island. An additional objective is to test further constant-offset and common-midpoint ground-penetrating radar as a non-invasive and inexpensive tools for tracking the position and shape of the water table and the fresh/saltwater transition both on the barrier island and at hydrologically significant sites on Long Island.

ACKNOWLEDGEMENTS

We would like to thank Vesna Kundic for her efforts in early stages of this work, John Lamprecht of LAWES for all of his help with drilling logistics, Tim Byrne of RMSP for help with field logistics, and all of our field assistants, including Kevin Hatton, Thomas Reilly, and the 'dynamic duo', Sara Foley and Kelsey Heynes.

REFERENCES:

Annan, A.P. *Ground Penetrating Radar Principles, Procedures, and Applications*, Sensors & Software Inc., 2003.

Baker, G.S. and Jol, H.M. (eds.), *Stratigraphic Analyses Using GPR*, Geological Society of America Special Paper 432, 2007

Buynevich, I. V., Jol, H.M., and Fitzgerald, D. *"Chapter 10: Costal Environments." Ground Penetrating Radar: Theory and Applications, Elsevier Science, 2008, pp. 299–322.*

Cooper, A., Green, A.N., and Loureiro, C., Geological constraints on mesoscale coastal barrier behavior, Global and Planetary Change. 168. 10.1016/j.gloplacha.2018.06.006, 2018

Girardi, J.D. and Davis, D.M., Parabolic dune reactivation and migration at Napeague, NY, USA: Insights from aerial and GPR imagery, Geomorphology 114. 530-541. 10.1016/j.geomorph.2009.08.011, 2010.

Grandfield. T and Davis. D.M., GPR as a Tool to Investigate the Three-Dimensional Structure of the Subsurface at Robert Moses State Park, Twenty-Seventh Conference on the Geology of Long Island and Metropolitan New York, 2020

Itzkin, M., A GPR-based Stratigraphic Analysis of Robert Moses State Park on Fire Island, New York, Senior Honors Thesis, Department of Geosciences, Stony Brook University, 2016.

Komar, Paul D. "Chapter 2: The Geomorphology of Eroding and Accreting Coasts." *Beach Processes and Sedimentation*, Prentice-Hall, 1998, pp. 25–38, 1998.

Neal, A., Ground-penetrating radar and its use in sedimentology: principles, problems and progress, *Earth-Science Reviews*, 66, 261-330, 2004.